



**HAL**  
open science

## Polyoxazolines based mixed micelles as PEG free formulations for an effective quercetin antioxidant topical delivery

L. Simon, M. Vincent, S. Le Saux, V. Lapinte, N. Marcotte, Marie Morille, C. Dorandeu, J.M. Devoisselle, S. Bégu

### ► To cite this version:

L. Simon, M. Vincent, S. Le Saux, V. Lapinte, N. Marcotte, et al.. Polyoxazolines based mixed micelles as PEG free formulations for an effective quercetin antioxidant topical delivery. *International Journal of Pharmaceutics*, 2019, 570, pp.118516. 10.1016/j.ijpharm.2019.118516 . hal-03212233

**HAL Id: hal-03212233**

**<https://hal.science/hal-03212233>**

Submitted on 20 Jul 2022

**HAL** is a multi-disciplinary open access archive for the deposit and dissemination of scientific research documents, whether they are published or not. The documents may come from teaching and research institutions in France or abroad, or from public or private research centers.

L'archive ouverte pluridisciplinaire **HAL**, est destinée au dépôt et à la diffusion de documents scientifiques de niveau recherche, publiés ou non, émanant des établissements d'enseignement et de recherche français ou étrangers, des laboratoires publics ou privés.



Distributed under a Creative Commons Attribution - NonCommercial 4.0 International License

1 Polyoxazolines based mixed micelles as PEG free formulations for an effective quercetin  
2 antioxidant topical delivery

3  
4 L. Simon, M. Vincent, S. Le Saux, V. Lapinte, N. Marcotte, M. Morille, C. Dorandeu, J.M. Devoisselle, S. Bégu<sup>\*</sup>  
5  
6 ICGM, Montpellier University, CNRS, ENSCM, Montpellier, France  
7

8

9 **1. Introduction**

10 With a surface of 2 m<sup>2</sup>, the skin is the most extended organ of the human body acting as barrier to mechanical  
11 and chemical aggressions (Marks and Miller, 2019). It plays a key role in protecting the body from daily toxic  
12 aggressions due to environmental pollutants by generating reactive oxygen species (ROS) (Valacchi et al., 2012).  
13 This overproduction of ROS unbalances the antioxidant defense system of the human body (Poljšak et al., 2011)  
14 leading to oxidative stress that can create skin damage like premature skin aging (Rinnerthaler et al., 2015) but  
15 also skin cancer risks (Baudouin et al., 2002). Among the environmental sources responsible for skin damage  
16 (Krutmann et al., 2017), UV radiations were unambiguously shown to cause skin cancers (Valacchi et al., 2012).  
17 UVAs were more especially identified to induce DNA mutations *in fine* generating skin carcinogenesis. Other  
18 environmental pollutants, such as polycyclic aromatic hydrocarbons, cigarette smoke constituents and ozone, are  
19 also considered today as accountable for skin pathologies and cutaneous cancers (Baudouin et al., 2002).  
20 To avoid the deleterious excess of ROS, antioxidant can be administrated through the skin. This topical delivery  
21 strategy uses natural or synthetic exogeneous molecules, with low or high molecular weight, as antioxidants  
22 (Andreia et al., 2011). Among all the natural compounds to be delivered, the highly lipophilic polyphenolic  
23 molecules belonging to the flavonoids family are often preferred for their powerful antioxidant properties and  
24 multiple pathways of activities (Nagula and Wairkar, 2019). Quercetin is one of the flavonols of interest for  
25 topical delivery since it gathers the properties of antioxidant and anti-inflammatory activities, wound healing and  
26 skin aging retardation. However, its low water solubility, instability to light and poor skin permeability (Hatahet  
27 et al., 2016a) require its formulation for an efficient activity. Therefore, various formulations such as smart  
28 crystals (Hatahet et al., 2016b), lipid nanocapsules (Hatahet et al., 2017), liposomes (Hatahet et al., 2018), solid  
29 lipid nanosystems (Bose et al., 2013), vesicles (Chessa et al., 2011), nanostructured lipid carriers (Chen-yu et al.,  
30 2012), nanoparticles (Tan et al., 2011), microemulsions (Martena et al., 2012) and lipid-based nanosystems  
31 (Caddeo et al., 2014) have been developed to enhanced the topical delivery of quercetin. It should be noted that  
32 most of these formulations use poly(ethylene glycol) (PEG) as stabilizer or thickener because of its very

33 interesting properties including biocompatibility, low toxicity, high solubility in aqueous media and stealth  
34 behavior. This explains the PEG overuse for cosmetic and pharmaceutical applications (Shen et al., 2018) and its  
35 success as the “gold standard” for drug delivery. Recently, clinical awareness on PEG overuse for oral and  
36 parenteral delivery pointed out safety issues associated with an increase of PEG antibodies (Lubich et al., 2016)  
37 and the possible accumulation of the polymer in body tissues (Rudmann et al., 2013), (Viegas et al., 2018).

38  
39 Therefore, researchers as well as companies are trying to find a polymer alternative to PEG. In this context, the  
40 poly(2-R-2-oxazoline)s (POx)s are investigated as one of the most suitable candidates. This polyamide family  
41 can be regarded as analogous of poly(amino acid)s with pseudo-peptidic structure. The biomedical properties of  
42 POx have been largely described in recent publications (Hoogenboom, 2009), (Adams and Schubert, 2007) or  
43 Lorson (Lorson et al., 2018). Its biocompatibility (Goddard et al., 1989), excellent cytocompatibility (Bauer et  
44 al., 2012) and hemocompatibility (Leiske et al., 2017) as well as the absence of accumulation in tissues and the  
45 rapid clearance from the bloodstream (Gaertner et al., 2007) have been emphasized. Moreover, the stealth  
46 behavior with suppression of the interactions with proteins and the immune system was proved (Zalipsky et al.,  
47 1996) allowing an immunocamouflage (Kyluik-Price et al., 2014). The most significant advance in biomedical  
48 POx concerns the recent results of Serina Therapeutics Inc. against Parkinson’s disease (Moreadith et al., 2017).  
49 They validated phase I clinical trials on POx based rotigotine conjugates whereas multi-dose trials are currently  
50 in progress to phase II.

51 Moreover, the versatility of POx can be noted with an easy additional functionalization when compared to PEG  
52 regarding the R pendent groups along the backbone (Verbraeken et al., 2017), (Guillerm et al., 2012b), (Guillerm  
53 et al., 2012a), (Korchia et al., 2015). Consequently, hydrophilic POx can be designed with methyl or ethyl R  
54 groups by contrast to hydrophobic POx with longer alkyl chains. Concerning poly(2-methyl-2-oxazoline), its  
55 more hydrophilic character than PEG and poly(2-ethyl-2-oxazoline) (Huber et al., 2008) offers an opportunity to  
56 elaborate amphiphilic (co)polymers contrasting with the hydrophobic block. In this way, to generate amphiphilic  
57 polymers, POx were associated with various hydrophobic blocks such as saturated or unsaturated lipids  
58 including fatty alcohols (El Asmar et al., 2016), fatty acids, triacyl glycerols (Stemmelen et al., 2013), (Giardi et  
59 al., 2009) or phospholipids (Purrucker et al., 2004).

60 With the aim of protecting active pharmaceutical ingredients (APIs), several types of nanocarriers based on POx  
61 physically incorporating an API have been described. These formulations include solid dispersions,  
62 nanoparticles and micelles in which various APIs (paclitaxel, curcumin, doxorubicine) have been solubilized

63 (Lorson et al., 2018). They were shown to be particularly interesting due to the limited number of steps required  
64 to synthesize the POx and the absence of necessity to tune the polymer towards the API as it is required for  
65 polymer-drug conjugates.

66 Regarding the association of POx and antioxidant API, little is reported in the literature. One can mention the  
67 conjugation of superoxide dismutase (SOD1) enzyme with POx to increase the release through the blood brain  
68 barrier and destroy superoxides (Yi and Kabanov, 2013). A radical fullerene-POx trap making use of the  
69 hydrophilicity of POx to disperse the anti-radical C60 molecules was also reported (Nukolova et al., 2011). A  
70 tribloc copolymer (PMeOx-*b*-PDMS-*b*-PMeOx) in polymersomes was shown to entrap a photosensitizer (rose  
71 bengal dye conjugated to bovine serum albumin) generating increased level of ROS by photodynamic therapy  
72 (Baumann et al., 2014), (Lorson et al., 2018).

73 To our knowledge, no POx topical formulation of flavonoids has been developed yet. In this context, a mixed  
74 nanosystem of POx and phospholipids for topical delivery was considered in this paper. Indeed, this hybrid  
75 system combines the features of liposomes and polymersomes by mixing the two components, i.e. the lipids and  
76 the amphiphilic copolymers, in a single vesicle. Either called hybrid polymer/lipid vesicle (Le Meins et al.,  
77 2013) or mixed micelles (Almgren, 2000), these systems have been studied over the past years and attracted  
78 attention for their versatile structure. It is notable that this mixture of lipid and polymer can lead to different  
79 nanostructures (D'Souza and Shegokar, 2016), such as core-shell of polymers and lipids (Mandal et al., 2013).  
80 Pippa *et al* have already worked on such hybrid nanosystems with POx and phospholipids for drug delivery  
81 systems and proved their efficacy as nanocontainers for the incorporation of therapeutic molecules (Pippa et al.,  
82 2013).

83 Herein, the investigated mixed-micelles were created based on phosphatidylcholine stabilized by an amphiphilic  
84 poly(2-methyl-2-oxazoline) bearing a long alkyl chain (Scheme 1). The stability and cell viability of these  
85 formulations were studied before and after being loaded with quercetin antioxidant. Then, the antioxidant  
86 activity of the loaded mixed micelles was measured. This work also aims to evaluate the potency of POx as an  
87 alternative to PEG in formulations.

88

89 **Scheme 1.** Schematic representation of the mixed-micelles loaded with quercetin.

90

## 91 **2. Materials and methods**

### 92 **Materials**

93

94 2-Methyl-2-oxazoline (MOx, Sigma Aldrich, 99.0%) was dried over CaH<sub>2</sub>, distilled at reduced pressure and  
95 stored under nitrogen atmosphere. Iodo-hexadecane (95.0 %), potassium hydroxide (KOH), quercetin (95%  
96 HPLC), phosphatidylcholine (L- $\alpha$ -Phosphatidylcholine from egg yolk  $\approx$  60%), Brij®58, DPPH (2,2-diphenyl-1-  
97 picrylhydrazyl), phenazine methosulfate (PMS), *tert*-Butyl hydroperoxide solution (TBHP) 70 % in water,  
98 acetonitrile, diethyl ether, methanol, acetone, phosphoric acid and 2,7-dichlorofluorescein diacetate (DCFDA)  
99 were purchased from Sigma Aldrich (Sigma Aldrich, Germany). Tween 80 (polysorbate 80) was purchased from  
100 BASF (BASF, Germany) and 3-(4,5-dimethylthiazol-2-yl)-5-(3-carboxymethoxyphenyl)-2-(4-sulfophenyl)-2H-  
101 tetrazolium, (MTS) from Promega (Promega, USA). MilliQ water was obtained from Milli-Q Gradient A10  
102 (Merck Millipore, Germany) apparatus.

103 Chloroform (for HPLC stabilized with ethanol) was bought from Carlo-Erba (Carlo Erba Reagent, Spain). All  
104 the reagents were used without further purification.

105 Spectra/Por 6 dialysis membranes pre-wetted RC tubing with 0.5-1 kDa MWCO were purchased from Spectrum  
106 Labs (Spectrum Labs, USA).

107

## 108 **Methods**

109

### 110 *2.1. Amphiphilic polyoxazolines synthesis (POx)*

111

112 POx synthesis was performed by cationic ring-opening polymerization of MOx. The polymerization was  
113 achieved under a nitrogen atmosphere after dissolving iodo-hexadecane (3.564 g, 10.1 mmol) and MOx (15 eq,  
114 151.7 mmol) in dry acetonitrile (0.5 M). The solution was vigorously stirred at 80 °C for 8 hours and then  
115 quenched by addition of potassium hydroxide dissolved in methanol (5 eq, 50.5 mmol, 5 M). The solution was  
116 stirred at 40 °C for additional 8 hours. The resulting polymer was isolated by precipitation by dropwise addition  
117 in cold diethyl ether and then filtration. The POx was then dialyzed with the dialysis membrane to eliminate  
118 residual diethyl ether and salts.

119

### 120 *2.2. Chemical characterization of POx*

121

122 Proton nuclear magnetic resonance ( $^1\text{H}$  NMR) spectra were recorded in  $\text{CDCl}_3$  a Bruker 400 MHz spectrometer.  
123 The POx exhibited the following shifts ( $\delta$ ) in reference to residual  $\text{CHCl}_3$  ( $\delta=7.26$  ppm), where (s) stands for  
124 singlet, (d) doublet, (t) triplet, (m) multiplet:  $\delta = 3.7\text{--}3.2$  (m,  $(4n + 2)\text{H}$ ,  $\text{CH}_2$  POx and  $\text{CH}_2$ Nalkyl chain), 2.4-2.1  
125 (m, 3n,  $\text{CH}_3$  POx), 1.3 (m, 20H,  $\text{CH}_2$  aliphatic), 0.9 (t, 3H,  $\text{CH}_3$  aliphatic).

126

### 127 *2.3. Critical aggregation concentration determination*

128

129 The critical aggregation concentration (CAC) of the POx was determined by surface tension measurements using  
130 the Wilhelmy plate method on K100 Krüss Processor Tensiometer from Krüss GmbH. A concentration range of  
131 polymer from 0.001 to 400 mg/L was prepared in MilliQ water. Prior to measurements, the solutions were kept  
132 under gentle stirring for 24 hours. Data were collected at 25 °C, a detection speed of 6 mm/min, detection  
133 sensitivity of 0.01 g and immersion depth of 2 mm using the Kruss software. A blank measurement was first  
134 performed using MilliQ water to ensure goodness of measure ( $\gamma= 69\text{--}73$  mN).

135

### 136 *2.4. Preparation of quercetin loaded mixed micelles (Q-MM)*

137

138 The mixed micelles (MM) were obtained by the thin film method developed by Bangham (Bangham et al.,  
139 1967). First phosphatidylcholine (PC), Polyoxazolines (POx) and quercetin (Q) were dissolved in a mixture of  
140 chloroform:acetone in 1:1 ratio, followed by the formation of thin film by evaporation of the solvent under  
141 vacuum. The film of mixed PC, POx and Q was hydrated by addition of filtered phosphate buffered saline (PBS,  
142 150 mM, pH 7.4). Nanosized MM were obtained following a high pressure homogenizer process of 5 cycles at  
143 10 000 PSI. Blank mixed micelles (B-MM) were prepared by the same method, except that quercetin was  
144 removed from the process.

145 Various molar ratios of Q: POx: PC were investigated from 3:1:10 to 7:1:50, after which the molar ratio 5:1:40  
146 was selected. It was optimized to ensure the smallest and most stable MM, with the lowest POx amount and the  
147 highest drug loading of quercetin.

148

### 149 *2.5. Photon correlation spectroscopy and electrophoretic mobility measurement*

150

151 Hydrodynamic diameter and polydispersity index (PDI) were measured using a Zetasizer NanoZS apparatus  
152 (Malvern Instruments, UK) equipped with a He-Ne laser (wavelength: 632.8 nm) at a temperature of 20 °C and a  
153 scattering angle of 173 ° for detection. Zeta potential was measured with 1000 µL of mixed micelles in  
154 disposable capillary cell (Malvern Instruments, UK). All the results are the average of three independent  
155 measurements.

156

#### 157 *2.6. Stability of Q-MM*

158

159 Blank and loaded MM samples were prepared and stored up to a month for stability study either at 4, 25 and 37  
160 °C for B-MM and at 4 °C only for Q-MM. The stability was evaluated from particle size and PDI measurements  
161 (see section 2.5) at day 0, 7, 14, 21, 28 for each temperature. The measurements were performed without  
162 filtration before measurements.

163 The stability of loaded mixed micelles was also evaluated using the concept of *in vitro* release by studying the  
164 concentration of quercetin diffusing through a nitrocellulose dialysis membrane from Q-MM to a receptor  
165 medium. The dialysis membrane was a 12 – 14 MWFC Spectra/Pore dialysis membrane (Spectrum laboratories,  
166 INC USA) and the receptor medium was composed of 40 mL PBS at pH 7.4 with 2 mass percent of Tween 80.  
167 The Q-MM were pre-filtered through 0.2 µm syringe filter (Whatman) to remove aggregated quercetin and then  
168 3 mL were incorporated into the membrane. The stability was determined at 25 °C after 1, 2, 3, 4, 5, 6 and 7  
169 hours. Quercetin concentration was determined by HPLC (section 2.9).

170

#### 171 *2.7. Transmission electron microscopy*

172

173 Transmission electron microscopy was performed on TEM Jeol 1400 PLUS (Jeol. Ltbd, Tokyo, Japan)  
174 associated with a camera Jeol 2K/2K. The samples previously diluted 10 times were deposited on grids type Cu  
175 formvar carbon and negatively stained with an aqueous uranyl acetate solution.

176

#### 177 *2.8. Differential Scanning Calorimetry (DSC)*

178

179 The crude quercetin powder and lyophilized Q-MM were analyzed by DSC using a Perkin Elmer DSC400  
180 apparatus (Perkin Elmer, USA).

181 The thermograms were recorded from 0 to 360 °C with a heating rate of 5 °C.min<sup>-1</sup>.

182

### 183 2.9. HPLC analysis

184

185 High Pressure Liquid Chromatography (HPLC) analysis of quercetin was performed on LC6-2012HT apparatus  
186 (Shimadzu, Kyoto, Japan) using a Prontosil C18 column (120-5-C18 H5.0 µm, 250x4.0 mm) as stationary phase.

187 The mobile phase was composed by a 40/60 volume ratio of acetonitrile to phosphoric acid solution at 0.2%  
188 mass at pH=1.9. The injection volume was 10µL and the flow rate was kept constant at 1 mL.min<sup>-1</sup> during the 10  
189 minutes of analysis. The detection was achieved using a UV-vis detector, (Shimadzu, Kyoto, Japan) at 368 nm  
190 (Yang et al., 2009). The calibration curve was performed with solutions of quercetin in methanol from 1 µg/mL  
191 to 100 µg/mL with a good linearity (r<sup>2</sup> = 0.9999).

192 The stability of quercetin in aqueous medium receptor (section 2.6) was established using a calibration curve of  
193 quercetin made in PBS buffer at pH 7.4 and Tween 80 (2% by mass) from 0.1 to 4 µg/mL (r<sup>2</sup> = 0.9996). The  
194 mobile phase, flow rate and detection wavelength remained unchanged.

195

### 196 2.10. Encapsulation efficacy (EE) and drug loading capacity (DL)

197

198 Quercetin loading capacity (DL) and encapsulation efficacy (EE) were determined by HPLC analysis as  
199 previously described (section 2.9) using 50 µL of the Q-MM sample solubilized in 950 µL methanol.

200 The amount of quercetin loaded (Eq.1) and the encapsulation efficacy (Eq.2) were calculated using the following  
201 equations:

202

$$203 \text{ Drug loading (\%)} = \frac{[\text{mass of quercetin}]}{[\text{total mass}]} \times 100 \quad (\text{Eq.1})$$

204

205

$$206 \text{ Encapsulation efficacy (\%)} = \frac{[\text{amount of encapsulated quercetin}]}{[\text{amount of quercetin initially loaded}]} \times 100 \quad (\text{Eq.2})$$

207

### 208 2.11. In vitro radical scavenging ability by 2,2-diphenyl-1-picrylhydrazyl (DPPH°)

209

210 The antioxidant activity of Q-MM loaded with quercetin was investigated by looking at the reactivity of  
211 quercetin with the free radical 2,2-diphenyl-1-picrylhydrazyl (DPPH°) (Blois, 1958). The antioxidant activity  
212 was determined by UV-visible spectroscopy from the decrease of the DPPH° radical absorbance at 517 nm using  
213 the following DPPH° scavenging equation (Eq.3):

214

215

$$216 \quad \text{DPPH}^\circ \text{ scavenging (\%)} = \frac{\text{Absorption of control} - \text{Absorption of sample}}{\text{Absorption of control}} \times 100 \quad (\text{Eq.3})$$

217

218 In which *absorption control* corresponds to the absorbance of 100 µM DPPH° solution. For the antioxidant  
219 activity test, the concentration of quercetin in Q-MM was set well below that of DPPH° at 2.5 ; 5 ; 7.5 ; 10 ; 12.5  
220 ; 15 µM.

221

#### 222 2.12. Cell culture

223

224 Mice fibroblasts cell line (NIH3T3) was purchased from American Type Cell Culture organization (USA). Cells  
225 were maintained in Dulbecco's Modified Eagle Medium (DMEM) (Gibco) supplemented with 10 % fetal bovine  
226 serum (Life Technologies), 1 % L-glutamine and 1 % penicillin/streptomycin equivalent to final concentration of  
227 2 nM for glutamine, 100 U.mL<sup>-1</sup> for penicillin and 100 µg.mL<sup>-1</sup> for streptomycin and incubated at 37 °C in  
228 humidified 5 % CO<sub>2</sub>.

229

#### 230 2.13. Cell viability

231

232 NIH3T3 cells were seeded at 20,000 cells/cm<sup>2</sup> in 96 well plate and incubated for 24 hours at 37 °C, 5 % CO<sub>2</sub> to  
233 allow cell adhesion. POx and Brij®58 at 40 g/L were solubilized in DMEM supplemented medium and filtered  
234 through 0.2 µm (no mass was lost through filtration).

235 Cells were treated or not (control) with POx or with the PEG reference (Brij®58) solutions at a concentration  
236 range from 0.01 to 20 g/L. After 24 hours of exposure, a CellTiter 96® Aqueous Non-Radioactive Cell  
237 Proliferation Assay (Promega, USA), was used to evaluate the cell viability following the manufacturer's  
238 instructions. The absorbance was then recorded at 490 nm using Multiskan™ GO Microplate Spectrophotometer  
239 (Thermo Scientific™, Waltham, Massachusetts, USA) and the background corresponding to wells free of cells

240 (mean of 3) was subtracted from each triplicate mean. Values of treated cells were normalized to non-treated  
241 cells (representing the 100 % cell viability).

242 Influence of a 24 hours treatment with B-MM, crude quercetin, or Q-MM solutions was also performed  
243 following the same protocol with quercetin concentrations of 1, 5, 10, 25, 50 µg/mL. The absorbance  
244 background of the formulations without cells was subtracted to the cellular tests.

245

246

#### 247 2.14. *Antioxidant effect of quercetin on NIH3T3 cells*

248

249 NIH3T3 cells were seeded at 20,000 cells/cm<sup>2</sup> in a 96 well black plate with clear bottom (Corning®  
250 Massachusetts, USA) and incubated 24 hours at 37 °C, 5 % CO<sub>2</sub> to allow cell adhesion. Then B-MM, crude  
251 quercetin, or Q-MM at a quercetin concentration of 5 µg/mL were added and incubated for another 24 hours in  
252 supplemented DMEM. Cells were washed twice with PBS before addition of 200 µL of 2,7-dichlorofluorescein  
253 diacetate (DCFDA) reagent (20 µM in DMEM without phenol red). A serum free media was used to avoid  
254 deacetylated the DCFDA from serum esterases into a non fluorescent compound, which can later be oxidized by  
255 ROS into DCF resulting in erroneous data.

256 After 30 minutes incubation at 37 °C, 5 % CO<sub>2</sub>, cells were washed with PBS and placed in 200 µL DMEM  
257 without phenol red. A solution of *tert*-Butyl hydroperoxide (TBHP) (500 µM in PBS) was then added and the  
258 cells were incubated for 30 additional minutes. The fluorescent signal of dichlorofluorescein (DCF) generated by  
259 the reaction of DCFDA reagent with ROS was then measured ( $\lambda_{exc}$  485 nm,  $\lambda_{em}$  535 nm) using Tristar LB941  
260 Spectrofluorimeter (Berthold Technologies, Germany). Values of treated cells were normalized to non-treated  
261 cells (representing the cells with 100 % ROS intensity).

262

#### 263 2.15. *Statistical analysis*

264

265 The statistical analysis of the data resulting from the cell viability and the antioxidant effect on cells was  
266 conducted with OriginPro software 8.1 (OriginLab, USA). A one-sample t-test with equal variance was  
267 performed to compare cell viability or antioxidant effect with formulations to viability of untreated cells (100  
268 %). A two-sample t-test with unequal variances was carried out to compare cell viability of formulations two by  
269 two. The P value reflects the significance with \* =P <0.05, \*\* =P <0.01 and \*\*\* =P < 0.001.



### 271 3. Results

#### 272 3.1. Synthesis of amphiphilic POx

273  
274 Amphiphilic POx considered as nonionic surfactants were synthesized from iodide initiators and potassium  
275 hydroxide as terminating agent (Scheme 2). The hydrophilic lipophilic balance (HLB) of the polymers depends  
276 on the length of the POx block predefined by the initial monomer/initiator molar ratio. In our case, 1-  
277 iodohexadecane was employed to elaborate C<sub>16</sub>POx<sub>15</sub> with narrow dispersity. The nonionic surfactant was well  
278 characterized by <sup>1</sup>H NMR spectroscopy with typical signals related to terminal CH<sub>3</sub> unit of hydrophobic block at  
279 0.85 ppm and the CH<sub>2</sub> of POx block at 3.2-3.7 ppm (see Figure 1S). The integration of these signals corresponds  
280 to the average degree of polymerization representing the length of the POx block, in our case 15, resulting in a  
281 molecular mass of the amphiphilic POx of 1520 g/mol and the measured critical aggregation concentration  
282 (CAC) of ~ 100 mg/L (66μM).

283 The chemistry of POx platform looks like the one of PEG using a ring-opening process of polymerization from  
284 cyclic monomer, 2-R-2-oxazoline for POx and ethylene oxide for PEG. However, the polymerization process  
285 differs for oxazolines with a cationic ring-opening polymerization (CROP) whereas for ethylene oxide an  
286 anionic one occurs. It should be noted that the high toxicity of ethylene oxide, gaseous at room temperature,  
287 required specific equipments and cautious handling which is not the case for oxazolines. To evaluate some of the  
288 POx surfactant properties, PEG surfactant named Brij<sup>®</sup>58 (reference) was selected based on its similar alkyl  
289 chain length alkyl chain (molar mass of 1125 g/mol) inducing an almost similar CAC (90 mg/L vs. 100mg/L) as  
290 it is the driving force of the self-assembly.

291

292 **Scheme 2.** Synthetic route of C<sub>16</sub>POx<sub>15</sub> and structure of the Brij<sup>®</sup>58 used as a reference

293

294 The surfactant properties of amphiphilic polymers in water were estimated by tensiometry measurements using  
295 the Wilhelmy plate method (Padday and Russell, 1960). It allows determining the critical aggregation  
296 concentration (CAC) value of surfactive molecules from the inflexion point occurring between a rapid decrease  
297 of surface tension at low concentrations and an almost constant value of the surface tension at higher  
298 concentrations. The CAC of C<sub>16</sub>POx<sub>15</sub> was thus estimated at 100 mg/L (65.9 μmol/L) (data not shown) at 25 °C.

299

#### 300 3.2. POx toxicity on NIH3T3 cells in comparison with PEG reference

301

302 The influence of POx (C<sub>16</sub>POx<sub>15</sub>) versus PEG reference (Brij®58) for a 24 hour treatment on NIH3T3 cell  
303 viability was conducted by treating cells with increasing concentrations from 0.01 to 20 g/L (Figure 1). Results  
304 were normalized to non treated cells (representing 100 %).

305 For concentrations ranging from 0.01 to 0.5 g/L no significant cell viability decrease was observed for both POx  
306 (C<sub>16</sub>POx<sub>15</sub>) and PEG reference (C<sub>16</sub>PEG<sub>20</sub>) By contrast, following a 0.1 g/L Brij®58 (C<sub>16</sub>PEG<sub>20</sub>) treatment, cell  
307 viability fell to 32 ± 3 % versus 112 ± 8 % for POx (C<sub>16</sub>POx<sub>15</sub>). A decrease of cell viability was observed for  
308 POx (C<sub>16</sub>POx<sub>15</sub>) to 60 ± 5 % only at 0.5 g/L. To summarize, following treatment from 0.1 to 0.2 g/L, POx has  
309 significantly (P < 0.001) less impact on cell viability than PEG reference. Interestingly, IC<sub>50</sub> (cellular viability) of the  
310 PEG amphiphilic reference was estimated at 0.090 g/L versus 0.75 g/L for amphiphilic POx.

311

312 **Figure 1.** Cell viability of mice fibroblast NIH3T3 co-incubated with increasing concentration of amphiphilic

313 POx (C<sub>16</sub>POx<sub>15</sub>) compared to amphiphilic PEG surfactant Brij® 58 (C<sub>16</sub>PEG<sub>20</sub>) for 24 h (n=3). Statistical

314 analysis was performed by a two-sample t-test between POx and PEG values (\*: P < 0.05, \*\*: P < 0.01 and \*\*\*:

315 P < 0.001).

316

317 *3.3. Particle size and surface charge of mixed micelles*

318

319 MM composed of PC and POx, with or without quercetin, were produced by thin film method and a high  
320 pressure homogenizer process (HPH) (Barnadas and Sabes, 2003). Table 1 summarized the average particle size  
321 and zeta potential of B-MM and Q-MM. The loading of the MM with quercetin did not influence their diameter  
322 with a particle diameter of 19±2 nm (Q-MM) instead of 18±2 nm without quercetin (B-MM). It can be noted  
323 that, no light scattering from crude quercetin, which tends to aggregate from 2.5 µg/mL in PBS, was observed in  
324 Q-MM solutions. The zeta potential for both blank and loaded MM was measured at 0 mV, indicating that the  
325 formulations had no charge at the surface.

326

327 **Table 1.** Mixed micelles structure characteristics.

328

329 *3.4. Morphology of mixed micelles*

330

331 The morphology of MM was investigated by transmission electron microscopy. Figure 2 shows typical images  
332 for Q-MM. Both B-MM and Q-MM exhibit a spherical shape and a similar size of about 20-30 nm. This is in  
333 agreement with the diameter of particles obtained from DLS analysis (Table 1).

334

335 **Figure 2 : TEM images for Q-MM**

336

337 *3.5. DSC analysis of Q-MM*

338

339 The crystallinity of quercetin as powder and once formulated in Q-MM was evaluated by differential scanning  
340 calorimetry, as illustrated in Figure 3. Before the Q-MM measurement, the formulation was concentrated twice  
341 and lyophilized. The crude quercetin exhibited two peaks, one at 155 °C and 323 °C, which are consistent with  
342 the literature. The first one is due to water evaporation (Pool et al., 2012) and the second one results from  
343 melting of the quercetin (Sahoo et al., 2011). The glass transition of POx only appears at 37 °C (Figure 2S). It is  
344 interesting to note that this glass transition was not observed on the Q-MM thermogram. More importantly, no  
345 peak for the quercetin crystallization could be observed. This indicates that nano-objects possess amorphous  
346 character, probably resulting from an homogeneous distribution of quercetin in the mixed micelle core.

347

348 **Figure 3: Thermograms properties of crude quercetin and Q-MM**

349

350 The difference of quercetin structure revealed by DSC was also observed on NIH3T3 mice fibroblasts cells 24  
351 hours after addition of the Q-MM and the crude quercetin to the cells. The quercetin concentration was  
352 equivalent in both experiments (50 µg/mL). Optical microscopy clearly revealed the presence of needles on  
353 NIH3T3 with quercetin only (Figure 4). Those were missing with Q-MM, i.e. once quercetin has been loaded in  
354 mixed micelles (Figure 4). This argues in favor of an homogenous distribution of quercetin in MM.

355

356 **Figure 4: Optical microscopy images of crude quercetin and Q-MM on NIH3T3 cells.**

357

358 *3.6. Formulation stability studies of B-MM and Q-MM*

359

360 The formulation stability of the B-MM was assessed over a month and evaluated every week at 4, 25 and 37 °C  
361 by analyzing the hydrodynamic diameter and polydispersity index (PDI) of MM using DLS experiments as  
362 shown in Figure 5. The B-MM remained stable over a month at each temperature, for example at 37 °C only a  
363 slight size increase from 24 nm to 31 nm with a  $PDI \leq 0.3$  was observed, thus indicating the good stability of the  
364 nano-formulations upon time and temperature.

365 As quercetin is very sensitive to thermal degradation, the Q-MM stability study was conducted at 4°C only. The  
366 particles were also stable over 14 days with no variation of the particle size from 26 nm on day 0 to 25 nm on  
367 day 28 with a PDI remaining at 0.3.

368

369 **Figure 5.** Particle size (column) and PDI (symbols) of B-MM at 4, 25, 37 °C (left) and Q-MM at 4 °C (right)  
370 over a month (n=3).

371

372 The stability of the Q-MM has also been evaluated through the release of quercetin over time, which should  
373 happen after decomposition on skin before the formulation had penetrated in the epidermis. To this end, a  
374 suspension of Q-MM was dialyzed in PBS buffer and in presence of Tween 20 (2% by mass) for 7 hours. A  
375 slight release of quercetin of only 6% was observed after 7 hours of dialysis (Figure 3S), confirming the above  
376 mentioned stability of the quercetin encapsulated MM formulations.

377

378 *3.7. Drug loading (DL) and encapsulation efficacy (EE) of Q-MM*

379

380 The drug loading (DL) and encapsulation efficiency (EE) for quercetin in Q-MM were calculated from HPLC  
381 analysis using the equations 1 and 2 described in section 2.10. DL reflects the amount of loaded quercetin  
382 relative to the total mass of the MM formulation, whereas EE represents the amount of quercetin experimentally  
383 encapsulated by comparison with the amount of quercetin added in solution. DL for this dermal delivery system  
384 was evaluated to  $3.6 \pm 0.2$  % corresponding to an EE of  $94 \pm 4$  %.

385

386 *3.8. Mixed micelles cellular viability on NIH3T3*

387

388 The cell viability test was performed on mice fibroblasts (NIH3T3) co-incubated with crude quercetin, B-MM  
389 and Q-MM at concentrations ranging from 1 to 50 µg/mL (Figure 6). Results were normalized to non-treated

390 cells (representing 100 %). After 24 hours, crude quercetin treatment induced a decrease in cell viability  
391 reaching  $72\pm9$  % at quercetin concentration of  $10\ \mu\text{g}/\text{mL}$ . By contrast no significant decrease in cell viability  
392 was observed when cells were treated with B-MM, at all concentrations. Interestingly, the quercetin encapsulated  
393 in MM showed less toxicity than the crude antioxidant at equivalent concentration of quercetin. For example at  
394  $25\ \mu\text{g}/\text{mL}$ , the crude quercetin cell viability was determined at  $33\pm17$  % and the one for Q-MM was twice higher  
395 at  $65\pm8$  %. The  $\text{IC}_{50}$  (cellular viability), was determined at  $17.5\ \mu\text{g}/\text{mL}$  for crude quercetin and  $37.5\ \mu\text{g}/\text{mL}$  for Q-MM  
396 evidencing a lower impact of quercetin on cell viability once encapsulated in Q-MM.

397

398 **Figure 6.** Cell viability of mice fibroblasts (NIH3T3) co-incubated with crude quercetin, B-MM and Q-MM for  
399 24 h (n=3). Statistical analysis was performed by a two-sample t-test between crude quercetin and B-MM, Q-  
400 MM (\*:  $P < 0.05$ , \*\*:  $P < 0.01$ ).

401

402 *3.9. Antioxidant effect*

403

404 *3.9.1. In vitro radical scavenging ability of Q-MM*

405

406 The radical scavenging ability of the crude quercetin and Q-MM was investigated with *in vitro* test using 2,2-  
407 diphenyl-1-picrylhydrazyl (DPPH $^\circ$ ) as a radical source. The quercetin antioxidant reacts with the free radical  
408 located at the hydrazine position of the DPPH $^\circ$ , thus leading to the reduced hydrazine form (DPPHH) and  
409 decreasing the amount of radicals. The DPPH test allowed to determine the  $\text{IC}_{50}$  (DPPH $^\circ$  inhibition) value: the  
410 concentration of quercetin for which 50 % of the DPPH $^\circ$  reacted. Figure 7 illustrates the DPPH $^\circ$  inhibition with  
411 quercetin concentration ranging from 2.5 to  $15\ \mu\text{M}$  for the free quercetin and encapsulated in MM (Q-MM). The  
412  $\text{IC}_{50}$  (DPPH $^\circ$  inhibition) values deduced from those measurements were  $9\ \mu\text{M}$  ( $3.6\ \mu\text{g}/\text{mL}$ ) for the free quercetin and  $6.5$   
413  $\mu\text{M}$  ( $2.6\ \mu\text{g}/\text{mL}$ ) for Q-MM. This indicates that the radical scavenging activity of quercetin was preserved upon  
414 encapsulation and even enhanced with respect to crude quercetin since its  $\text{IC}_{50}$  value was lower.

415

416 **Figure 7.** DPPH $^\circ$  inhibition of free quercetin and Q-MM with quercetin concentration

417

418 *3.9.2. Cellular testing on NIH3T3 with TBHP*

419

420 The antioxidant activity of the Q-MM was tested on mice fibroblasts (NIH3T3) in comparison with crude  
421 quercetin and B-MM (Figure 8). A quercetin concentration of 5 µg/mL was selected as no decrease in cell  
422 viability was observed regardless of the formulation.

423 Cells were first treated with formulations for 24 hours before being washed and labeled with 2,7-  
424 dichlorofluorescein (DCFDA). The oxidative stress was then induced by *tert*-butyl hydroperoxide (TBHP) for 30  
425 minutes before measuring the fluorescence intensity signal. A serum free medium was used to avoid  
426 deacetylated the DCFDA from serum esterases into a non fluorescent compound, which can later be oxidized by  
427 ROS into DCF resulting in erroneous data.

428 The results were normalized to TBHP treated cells (positive control) and the untreated cells were set as negative  
429 control. The addition of TBHP increased the ROS generated by 25±2 % (P < 0.001) compared to negative  
430 control. The crude quercetin and Q-MM formulation significantly reduced generated ROS by 36±3 % and by  
431 42±2 % respectively compared to cells treated with TBHP. The antioxidant activity of the quercetin was  
432 maintained once formulated in MM. No significant difference in the antioxidant activity of crude quercetin  
433 versus Q-MM was evidenced.

434 Therefore Q-MM was able to scavenge the excess of ROS allowing a recovery to basal ROS concentration  
435 values. The antioxidant effect of the Q-MM seems to be only due to the quercetin encapsulated in the  
436 formulation as the ability of B-MM to reduce ROS was very low.

437

438 **Figure 8.** ROS relative intensity for crude quercetin, B-MM and Q-MM (quercetin concentration 5 µg/mL)  
439 (n=3). Negative control was untreated cells (without TBHP or formulations) and positive control was cells  
440 treated with TBHP without formulation. Fluorescent intensity was normalized to TBHP treated cells (positive  
441 control). A one sample t-test relative to positive control cells was performed (\*: P < 0.05, \*\*: P < 0.01 and \*\*\*:  
442 P < 0.001).

443

444

445

#### 446 4. Discussion

447 Two aspects were investigated in this study: (i) the stability of mixed micelles formulated with POx as  
448 alternative to PEG and (ii) quercetin loading and quercetin antioxidant efficiency in these POx-formulations (Q-  
449 MM). Among all the previously developed formulations for topical delivery of quercetin (Hatahet et al., 2018),  
450 mixed micelles were selected as the first proof of concept for antioxidant POx-formulations. These formulations  
451 were constituted of phosphatidylcholine and an amphiphilic poly(2-methyl-2-oxazoline) molecule bearing a long  
452 alkyl chain (POx, C<sub>16</sub>POx<sub>15</sub>).

453 The surfactant property of POx itself was first evaluated. It presents a critical aggregation concentration (CAC)  
454 of ~ 100 mg/L, which is similar to structural analogue Brij®58 used as a reference. In contrast, the impact of the  
455 two amphiphilic molecules on cell viability was very different. A better cell viability in presence of POx (Figure  
456 1) was highlighted with a IC<sub>50 (cellular viability)</sub> of 0.75 g/L compared to 0.09 g/L for Brij®58. The POx concentration  
457 for formulation of mixed micelles was about 50 times under the IC<sub>50 (cellular viability)</sub> of POx, ensuring non toxic  
458 working conditions. Therefore, POx was proved to have significantly (P < 0.001) less impact on cell viability  
459 than its PEG equivalent. These results are consistent with the literature since the polyoxazolines polymer family  
460 is known to have an excellent cytocompatibility and hemocompatibility (Lorson et al., 2018). However, it is the  
461 first time that an amphiphilic POx with such architecture (C<sub>16</sub>POx<sub>15</sub>) was investigated. Then, this amphiphilic  
462 POx was associated with phospholipids to increase the solubility of hydrophobic antioxidant within the micelles.  
463 The mixed micelles of phosphatidylcholine stabilized by C<sub>16</sub>POx<sub>15</sub> (B-MM) were produced using thin film  
464 process. After a high pressure homogenization, the formulation presented a reduced homogeneous particle size  
465 of 18±2 nm (Figure 2). These DLS and CAC results confirmed that nanosized mixed-micelles were created and  
466 not POx micelles and liposomes coexisting.

467 The same process was used in the presence of quercetin, leading to an excellent encapsulation efficiency that  
468 reached up to 94±4 %. This allowed a particularly high concentration of antioxidant in the formulations to be  
469 loaded (3.6±0.17 %), which reached 188 µg/ml in Q-MM instead of 2.48 µg/ml in PBS. It was shown that  
470 neither the spherical shape nor the particle size of MM were modified upon loading with quercetin (Q-MM)  
471 (Table 1). This contrasts with the existing hybrid nanosystems DPPC : MPOx (Pippa et al., 2013) for which the  
472 incorporation of indomethacin (with the same molar mass as quercetin and the same nature of polycyclic  
473 aromatic ring) induced a significant size increase. The incorporation efficiency was also significantly lower with  
474 a maximum of 17 %. Looking at some others lipid formulations for topical delivery of quercetin the  
475 encapsulation efficiency, drug loading and particle size reached with the Q-MM (94 %, 3.6 %, 19 nm), are more

476 satisfactory than nanostructured lipid carriers (89.95 %, 3.05 %, 215.2 nm) (Chen-yu et al., 2012), phospholipids  
477 based vesicles (48-75 %, NV (no value), 80-220 nm) (Chessa et al., 2011), lecithin-chitosan nanoparticles (48.5  
478 %, 2.45 %, 100 nm) (Tan et al., 2011), and nanovesicles (81-91 %, NV, 80-110 nm) (Manca et al., 2014).  
479 Moreover, the nanometric size obtained for the MM formulation is particularly interesting since it is known to  
480 ensure enhanced penetration into skin (Schäfer-Korting et al., 2007).

481 Concerning the quercetin dispersion in Q-MM, a thermal analysis performed by DSC corroborated by  
482 microscopy (Figure 4) indicated that quercetin was well dispersed in the core of Q-MM, losing its crystalline  
483 character in favor of an amorphous phase (Pool et al., 2012), (Sahoo et al., 2011). This feature also indicates that  
484 once the Q-MM has penetrated into skin, quercetin should be easily released out of the formulation.

485 To evaluate POx formulation stability, the size and PDI of B-MM and Q-MM were measured every week at  
486 various temperatures (4, 25 and 37 °C) for 28 days. B-MM remained stable at all 3 temperatures reflecting the  
487 high stabilizing capacity of POx. Regarding Q-MM, since quercetin is very sensitive to thermal degradation  
488 (Wang and Zhao, 2016) even at 25 and 37 °C leading overtime to antioxidant degradation into intermediate  
489 products, the stability study was only conducted at storage condition 4°C, as also performed by Bose et al (Bose  
490 et al., 2013). The size of Q-MM remained around 26 nm over 14 days with a PDI under 0.3. The PDI increase  
491 after 14 days might be due to the quercetin loading as it was not the case for B-MM. This formulation could be  
492 more stable once loaded with another active compound. MM thus represents a quite stable quercetin formulation  
493 as a low quantity of quercetin (less than 6%) was released *in vitro* from the formulation over 7 hours. All the  
494 results demonstrated the efficiency of POx to stabilize MM formulation and its ability to load a large amount of  
495 antioxidants such as quercetin, indicating this formulation is promising for topical application. Indeed, the lipid  
496 composition of the MM along with the presence of POx could facilitate the delivery of quercetin in the skin  
497 epidermis (Ashtikar et al., 2016), (Casiraghi et al., 2015).

498  
499 The cellular viability of crude quercetin, B-MM and Q-MM was evaluated on mice fibroblasts after 24 hours of  
500 exposure. With a quercetin concentration from 10 to 25 µg/mL, cell viability dropped from 72±9 % to 33±17 %  
501 for crude quercetin whereas a slighter decrease for Q-MM (from 82±10 % to 62±8 %) was observed (Figure 6).  
502 This evidenced the interest of quercetin in association with MM. This statement is also highlighted by difference  
503 in IC<sub>50</sub> (cellular viability) values, as crude quercetin has a value twice higher than Q-MM (17.5 µg/mL versus 37.5  
504 µg/mL respectively). Moreover, it has been confirmed that the effect of Q-MM was only due to the quercetin  
505 itself as B-MM had no impact on cell viability. These results confirmed the cell viability study of polyoxazolines

506 (Figure 1) in which POx had no impact on cell viability over a broad concentration range including the one used  
507 for MM formulation (about 15 mg/L). MM formulations were concentrated enough in quercetin so their  
508 antioxidant efficacy could be evaluated.

509 The antioxidant activity of Q-MM related to crude quercetin was first evaluated *in vitro* using DPPH assay, to  
510 ensure that the radical scavenging activity of quercetin was preserved and was even enhanced once encapsulated.  
511 The IC<sub>50</sub> (DPPH<sup>•</sup> inhibition) value of Q-MM compared to crude quercetin decreased from 9 to 6.5 μM (equivalent to  
512 3.6 to 2.6 μg/mL). The Q-MM antioxidant capacity also relies on POx being more stable regarding oxidative  
513 degradation compared to PEG: the polyether backbone is more prone to oxidative degradation (Ostuni et al.,  
514 2001). To evaluate the ability of quercetin to counteract the oxidative stress induced by ROS, mice fibroblasts  
515 were used as a cellular model with an oxidative stress induced by TBHP. The antioxidant efficacy of the  
516 quercetin was maintained once encapsulated in Q-MM. By comparison, crude quercetin was able to reduced the  
517 ROS generated by TBHP by 36 % whereas Q-MM decreased them by 42 % (Figure 8). Moreover, Q-MM was  
518 able to scavenge the excess of ROS allowing a recovery to basal ROS concentration values (about 75% as  
519 measured with untreated cells). Since the toxicity of Q-MM was lower than crude quercetin, the concentration  
520 for the antioxidant test could be increased for a potentially even higher efficacy on cells.

521

## 522 **5. Conclusion**

523 This study on amphiphilic polyoxazolines (C<sub>16</sub>POx<sub>15</sub>) provides insight into the great promise this polymer family  
524 holds for the development of pharmaceutical and cosmetic formulations. The higher cell viability (at a similar  
525 CAC value) compared to Brij®58, a worldwide used industrial nonionic surfactant, demonstrates the potential of  
526 this POx family in the formulation of API. The ability of the amphiphilic POx to produce stable formulations  
527 was investigated for the first time with mixed micelles of POx and phosphatidylcholine using thin film and HPH  
528 process. DLS and TEM measurements showed spherical micelles of around 18 nm without API (B-MM) and no  
529 size increase once loaded in a natural antioxidant quercetin (Q-MM). These mixed-micelles were stable over 28  
530 days and present a long-lasting encapsulation with less than 6% release over 7 hours. Moreover, a good quercetin  
531 encapsulation (94±4 %) efficiency was measured with these nanosystems allowing its homogeneous  
532 solubilization in the core under amorphous character. Therefore, Q-MM can be used as a reservoir of quercetin.  
533 Once loaded in the MM, the quercetin impact on cell viability was twice reduced while the quercetin antioxidant  
534 efficacy was preserved. Q-MM was able to reduce by 42 % of the ROS generated by TBHP allowing a recovery  
535 to basal ROS concentration values.

536 Optimal features such as composition, size, stability, encapsulation efficiency, preservation of antioxidant  
537 activity are brought together in the mixed micelles, a very promising formulation for an effective topical delivery  
538 to the deepest layer of the epidermis. Future studies will focus on the evaluation of the penetration capacity of  
539 amphiphilic polyoxazolines and Q-MM and the topical delivery of quercetin in *in vivo* testing.

540

541

542

543

544

545

546

547

548

549

550

551

552

553

554

555 **Supplementary information**

556 **Figure 1S.** NMR Spectrum of C<sub>16</sub>POx<sub>15</sub>

557

558 **Figure 2S.** DSC curve of C<sub>16</sub>POx<sub>15</sub> at 20 °C.min<sup>-1</sup>

559

560 **Figure 3S.** Quercetin release of loaded MM related to time.

561

562 **References**

- 563 **Adams, N., Schubert, U.S., 2007. Poly(2-oxazolines) in biological and biomedical application**  
564 **contexts. *Advanced Drug Delivery Reviews* 59, 1504-1520.**
- 565 **Almgren, M., 2000. Mixed micelles and other structures in the solubilization of bilayer lipid**  
566 **membranes by surfactants. *Biochimica et Biophysica Acta (BBA) - Biomembranes* 1508, 146-163.**
- 567 **Andreia, A., Helena Margarida, R., Helena Cabral, M., Sandra, S., 2011. Topical Delivery of**  
568 **Antioxidants. *Current Drug Delivery* 8, 640-660.**
- 569 **Ashtikar, M., Nagarsekar, K., Fahr, A., 2016. Transdermal delivery from liposomal formulations –**  
570 **Evolution of the technology over the last three decades. *Journal of Controlled Release* 242, 126-**  
571 **140.**
- 572 **Bangham, A.D., De Gier, J., Greville, G.D., 1967. Osmotic Properties and Water Permeability of**  
573 **Phospholipid Liquid Crystals.**
- 574 **Barnadas, R.R., Sabes, X.M., 2003. Liposomes prepared by high-pressure homogenizers.**
- 575 **Baudouin, C., Charveron, M., Tarroux, R., Gall, Y., 2002. Environmental pollutants and skin cancer.**  
576 ***Cell Biology and Toxicology* 18, 341-348.**
- 577 **Bauer, M., Lautenschlaeger, C., Kempe, K., Tauhardt, L., Schubert, U.S., Fischer, D., 2012. Poly(2-**  
578 **ethyl-2-oxazoline) as Alternative for the Stealth Polymer Poly(ethylene glycol): Comparison of in**  
579 **vitro Cytotoxicity and Hemocompatibility. *Macromolecular Bioscience* 12, 986-998.**
- 580 **Baumann, P., Spulber, M., Dinu, I.A., Palivan, C.G., 2014. Cellular Trojan Horse Based Polymer**  
581 **Nanoreactors with Light-Sensitive Activity. *The Journal of Physical Chemistry B* 118, 9361-9370.**
- 582 **Blois, M.S., 1958. Antioxidant Determinations by the Use of a Stable Free Radical. *Nature* 181,**  
583 **1199-1200.**
- 584 **Bose, S., Du, Y., Takhistov, P., Michniak-Kohn, B., 2013. Formulation optimization and topical**  
585 **delivery of quercetin from solid lipid based nanosystems. *International Journal of Pharmaceutics***  
586 **441, 56-66.**

587 Caddeo, C., Díez-Sales, O., Pons, R., Fernández-Busquets, X., Fadda, A.M., Manconi, M., 2014.  
588 Topical Anti-Inflammatory Potential of Quercetin in Lipid-Based Nanosystems: In Vivo and In Vitro  
589 Evaluation. *Pharmaceutical Research* 31, 959-968.

590 Casiraghi, A., Selmin, F., Minghetti, P., Cilurzo, F., Montanari, L., 2015. Nonionic Surfactants:  
591 Polyethylene Glycol (PEG) Ethers and Fatty Acid Esters as Penetration Enhancers, in: Dragicevic, N.,  
592 Maibach, H.I. (Eds.), *Percutaneous Penetration Enhancers Chemical Methods in Penetration*  
593 *Enhancement: Modification of the Stratum Corneum*. Springer Berlin Heidelberg, Berlin,  
594 Heidelberg, pp. 251-271.

595 Chen-yu, G., Chun-fen, Y., Qi-lu, L., Qi, T., Yan-wei, X., Wei-na, L., Guang-xi, Z., 2012. Development  
596 of a Quercetin-loaded nanostructured lipid carrier formulation for topical delivery. *International*  
597 *Journal of Pharmaceutics* 430, 292-298.

598 Chessa, M., Caddeo, C., Valenti, D., Manconi, M., Sinico, C., Fadda, A.M., 2011. Effect of  
599 Penetration Enhancer Containing Vesicles on the Percutaneous Delivery of Quercetin through New  
600 Born Pig Skin. *Pharmaceutics* 3, 497-509.

601 D'Souza, A., Shegokar, R., 2016. Polymer: Lipid Hybrid Nanostructures in Cancer Drug Delivery:  
602 Successes and Limitations, pp. 431-463.

603 El Asmar, A., Gimello, O., Morandi, G., Le Cerf, D., Lapinte, V., Burel, F., 2016. Tuning the Thermo-  
604 Sensitivity of Micellar Systems through a Blending Approach. *Macromolecules* 49, 4307-4315.

605 Gaertner, F.C., Luxenhofer, R., Blechert, B., Jordan, R., Essler, M., 2007. Synthesis, biodistribution  
606 and excretion of radiolabeled poly(2-alkyl-2-oxazoline)s. *Journal of Controlled Release* 119, 291-  
607 300.

608 Giardi, C., Lapinte, V., Charnay, C., Robin, J.J., 2009. Nonionic polyoxazoline surfactants based on  
609 renewable source: Synthesis, surface and bulk properties. *Reactive and Functional Polymers* 69,  
610 643-649.

611 **Goddard, P., Hutchinson, L.E., Brown, J., Brookman, L.J., 1989. Soluble polymeric carriers for drug**  
612 **delivery. Part 2. Preparation and in vivo behaviour of N-acylethylenimine copolymers. Journal of**  
613 **Controlled Release 10, 5-16.**

614 **Guillerm, B., Darcos, V., Lapinte, V., Monge, S., Coudane, J., Robin, J.-J., 2012a. Synthesis and**  
615 **evaluation of triazole-linked poly( $\epsilon$ -caprolactone)-graft-poly(2-methyl-2-oxazoline) copolymers as**  
616 **potential drug carriers. Chemical Communications 48, 2879-2881.**

617 **Guillerm, B., Monge, S., Lapinte, V., Robin, J.-J., 2012b. How to Modulate the Chemical Structure of**  
618 **Polyoxazolines by Appropriate Functionalization. Macromolecular Rapid Communications 33,**  
619 **1600-1612.**

620 **Hatahet, T., Morille, M., Hommoss, A., Devoisselle, J.M., Müller, R.H., Bégu, S., 2016a. Quercetin**  
621 **topical application, from conventional dosage forms to nanodosage forms. European Journal of**  
622 **Pharmaceutics and Biopharmaceutics 108, 41-53.**

623 **Hatahet, T., Morille, M., Hommoss, A., Devoisselle, J.M., Müller, R.H., Bégu, S., 2018. Liposomes,**  
624 **lipid nanocapsules and smartCrystals<sup>®</sup>: A comparative study for an effective quercetin delivery to**  
625 **the skin. International Journal of Pharmaceutics 542, 176-185.**

626 **Hatahet, T., Morille, M., Hommoss, A., Dorandeu, C., Müller, R.H., Bégu, S., 2016b. Dermal**  
627 **quercetin smartCrystals<sup>®</sup>: Formulation development, antioxidant activity and cellular safety.**  
628 **European Journal of Pharmaceutics and Biopharmaceutics 102, 51-63.**

629 **Hatahet, T., Morille, M., Shamseddin, A., Aubert-Pouëssel, A., Devoisselle, J.M., Bégu, S., 2017.**  
630 **Dermal quercetin lipid nanocapsules: Influence of the formulation on antioxidant activity and**  
631 **cellular protection against hydrogen peroxide. International Journal of Pharmaceutics 518, 167-**  
632 **176.**

633 **Hoogenboom, R., 2009. Poly(2-oxazoline)s: A Polymer Class with Numerous Potential Applications.**  
634 **Angewandte Chemie International Edition 48, 7978-7994.**

635 **Huber, S., Hutter, N., Jordan, R., 2008. Effect of end group polarity upon the lower critical solution**  
636 **temperature of poly(2-isopropyl-2-oxazoline).**

637 Korchia, L., Bouilhac, C., Lapinte, V., Travelet, C., Borsali, R., Robin, J.-J., 2015. Photodimerization as  
638 an alternative to photocrosslinking of nanoparticles: proof of concept with amphiphilic linear  
639 polyoxazoline bearing coumarin unit. *Polymer Chemistry* 6, 6029-6039.

640 Krutmann, J., Bouloc, A., Sore, G., Bernard, B.A., Passeron, T., 2017. The skin aging exposome.  
641 *Journal of Dermatological Science* 85, 152-161.

642 Kyliuk-Price, D.L., Li, L., Scott, M.D., 2014. Comparative efficacy of blood cell immunocamouflage  
643 by membrane grafting of methoxypoly(ethylene glycol) and polyethyloxazoline. *Biomaterials* 35,  
644 412-422.

645 Le Meins, J.F., Schatz, C., Lecommandoux, S., Sandre, O., 2013. Hybrid polymer/lipid vesicles: state  
646 of the art and future perspectives. *Materials Today* 16, 397-402.

647 Leiske, M.N., Trützscher, A.-K., Armoneit, S., Sungur, P., Hoepfner, S., Lehmann, M., Traeger, A.,  
648 Schubert, U.S., 2017. Mission ImPOxable – or the unknown utilization of non-toxic poly(2-  
649 oxazoline)s as cryoprotectants and surfactants at the same time. *Journal of Materials Chemistry B*  
650 5, 9102-9113.

651 Lorson, T., Lübtow, M.M., Wegener, E., Haider, M.S., Borova, S., Nahm, D., Jordan, R., Sokolski-  
652 Papkov, M., Kabanov, A.V., Luxenhofer, R., 2018. Poly(2-oxazoline)s based biomaterials: A  
653 comprehensive and critical update. *Biomaterials* 178, 204-280.

654 Lubich, C., Allacher, P., de la Rosa, M., Bauer, A., Prenninger, T., Horling, F.M., Siekmann, J.,  
655 Oldenburg, J., Scheiflinger, F., Reipert, B.M., 2016. The Mystery of Antibodies Against Polyethylene  
656 Glycol (PEG) - What do we Know? *Pharmaceutical Research* 33, 2239-2249.

657 Manca, M.L., Castangia, I., Caddeo, C., Pando, D., Escribano, E., Valenti, D., Lampis, S., Zaru, M.,  
658 Fadda, A.M., Manconi, M., 2014. Improvement of quercetin protective effect against oxidative  
659 stress skin damages by incorporation in nanovesicles. *Colloids and Surfaces B: Biointerfaces* 123,  
660 566-574.

661 **Mandal, B., Bhattacharjee, H., Mittal, N., Sah, H., Balabathula, P., Thoma, L.A., Wood, G.C., 2013.**  
662 **Core–shell-type lipid–polymer hybrid nanoparticles as a drug delivery platform. *Nanomedicine:***  
663 ***Nanotechnology, Biology and Medicine* 9, 474-491.**

664 **Marks, J.G., Miller, J.J., 2019. 2 - Structure and Function of the Skin, in: Marks, J.G., Miller, J.J.**  
665 **(Eds.), *Lookingbill and Marks' Principles of Dermatology (Sixth Edition)*. Content Repository Only!,**  
666 **London, pp. 2-10.**

667 **Martena, V., Hoti, E., Malaj, L., Di Martino, P., 2012. Permeation and skin retention of quercetin**  
668 **from microemulsions containing Transcutol® P AU - Censi, Roberta. *Drug Development and***  
669 ***Industrial Pharmacy* 38, 1128-1133.**

670 **Moreadith, R.W., Viegas, T.X., Bentley, M.D., Harris, J.M., Fang, Z., Yoon, K., Dizman, B., Weimer,**  
671 **R., Rae, B.P., Li, X., Rader, C., Standaert, D., Olanow, W., 2017. Clinical development of a poly(2-**  
672 **oxazoline) (POZ) polymer therapeutic for the treatment of Parkinson’s disease – Proof of concept**  
673 **of POZ as a versatile polymer platform for drug development in multiple therapeutic indications.**  
674 ***European Polymer Journal* 88, 524-552.**

675 **Nagula, R.L., Wairkar, S., 2019. Recent advances in topical delivery of flavonoids: A review. *Journal***  
676 ***of Controlled Release* 296, 190-201.**

677 **Nukolova, N.V., Oberoi, H.S., Cohen, S.M., Kabanov, A.V., Bronich, T.K., 2011. Folate-decorated**  
678 **nanogels for targeted therapy of ovarian cancer. *Biomaterials* 32, 5417-5426.**

679 **Ostuni, E., Chapman, R.G., Holmlin, R.E., Takayama, S., Whitesides, G.M., 2001. A Survey of**  
680 **Structure–Property Relationships of Surfaces that Resist the Adsorption of Protein. *Langmuir* 17,**  
681 **5605-5620.**

682 **Padday, J.F., Russell, D.R., 1960. The measurement of the surface tension of pure liquids and**  
683 **solutions. *Journal of Colloid Science* 15, 503-511.**

684 **Pippa, N., Merkouraki, M., Pispas, S., Demetzos, C., 2013. DPPC:MPOx chimeric advanced Drug**  
685 **Delivery nano Systems (chi-aDDnSs): Physicochemical and structural characterization, stability and**  
686 **drug release studies. *International Journal of Pharmaceutics* 450, 1-10.**

687 Poljšak, B., Glavan, U., Dahmane, R., 2011. Skin Cancer, Free Radicals and Antioxidants.

688 Pool, H., Quintanar, D., Figueroa, J.d.D., Marinho Mano, C., Bechara, J.E.H., God, #xed, nez, L.A.,

689 Mendoza, S., 2012. Antioxidant Effects of Quercetin and Catechin Encapsulated into PLGA

690 Nanoparticles. *Journal of Nanomaterials* 2012, 12.

691 Purrucker, O., Förtig, A., Jordan, R., Tanaka, M., 2004. Supported Membranes with Well-Defined

692 Polymer Tethers—Incorporation of Cell Receptors. *ChemPhysChem* 5, 327-335.

693 Rinnerthaler, M., Bischof, J., Streubel, M.K., Trost, A., Richter, K., 2015. Oxidative stress in aging

694 human skin. *Biomolecules* 5, 545-589.

695 Rudmann, D.G., Alston, J.T., Hanson, J.C., Heidel, S., 2013. High Molecular Weight Polyethylene

696 Glycol Cellular Distribution and PEG-associated Cytoplasmic Vacuolation Is Molecular Weight

697 Dependent and Does Not Require Conjugation to Proteins. *Toxicologic Pathology* 41, 970-983.

698 Sahoo, N.G., Kakran, M., Shaal, L.A., Li, L., Müller, R.H., Pal, M., Tan, L.P., 2011. Preparation and

699 Characterization of Quercetin Nanocrystals. *Journal of Pharmaceutical Sciences* 100, 2379-2390.

700 Schäfer-Korting, M., Mehnert, W., Korting, H.-C., 2007. Lipid nanoparticles for improved topical

701 application of drugs for skin diseases. *Advanced Drug Delivery Reviews* 59, 427-443.

702 Shen, Z., Fisher, A., Liu, W.K., Li, Y., 2018. 1 - PEGylated “stealth” nanoparticles and liposomes, in:

703 Parambath, A. (Ed.), *Engineering of Biomaterials for Drug Delivery Systems*. Woodhead Publishing,

704 pp. 1-26.

705 Stemmelen, M., Travelet, C., Lapinte, V., Borsali, R., Robin, J.-J., 2013. Synthesis and self-assembly

706 of amphiphilic polymers based on polyoxazoline and vegetable oil derivatives. *Polymer Chemistry*

707 4, 1445-1458.

708 Tan, Q., Liu, W., Guo, C., Zhai, G., 2011. Preparation and evaluation of quercetin-loaded lecithin-

709 chitosan nanoparticles for topical delivery. *International journal of nanomedicine* 6, 1621-1630.

710 Valacchi, G., Sticozzi, C., Pecorelli, A., Cervellati, F., Cervellati, C., Maioli, E., 2012. Cutaneous

711 responses to environmental stressors. *Annals of the New York Academy of Sciences* 1271, 75-81.

712 Verbraeken, B., Monnery, B.D., Lava, K., Hoogenboom, R., 2017. The chemistry of poly(2-  
713 oxazoline)s. *European Polymer Journal* 88, 451-469.

714 Viegas, T.X., Fang, Z., Yoon, K., Weimer, R., Dizman, B., 2018. 6 - Poly(oxazolines), in: Parambath, A.  
715 (Ed.), *Engineering of Biomaterials for Drug Delivery Systems*. Woodhead Publishing, pp. 173-198.

716 Wang, J., Zhao, X.H., 2016. Degradation kinetics of fisetin and quercetin in solutions affected by  
717 medium pH, temperature and co-existing proteins. *Journal of the Serbian Chemical Society* 81, 243-  
718 254.

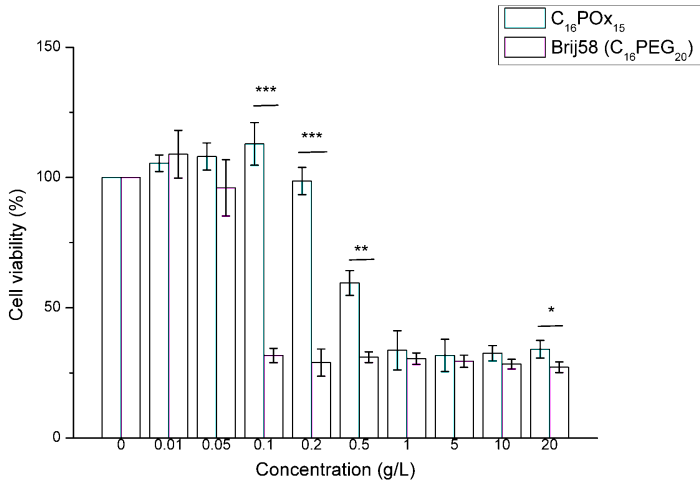
719 Yang, L., Li, P., Gao, Y.-J., Li, H.-F., Wu, D.-C., Li, R.-X., 2009. Time Resolved UV-Vis Absorption  
720 Spectra of Quercetin Reacting with Various Concentrations of Sodium Hydroxide.

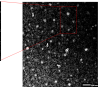
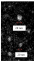
721 Yi, X., Kabanov, A.V., 2013. Brain delivery of proteins via their fatty acid and block copolymer  
722 modifications. *Journal of drug targeting* 21, 940-955.

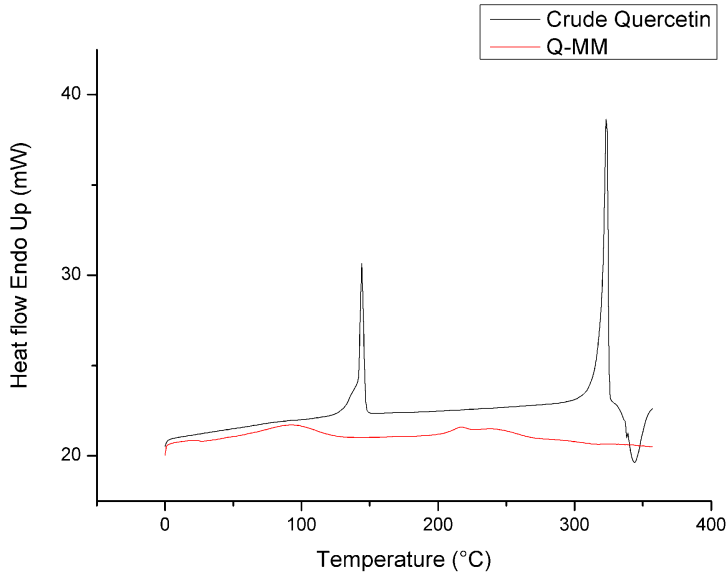
723 Zalipsky, S., Hansen, C.B., Oaks, J.M., Allen, T.M., 1996. Evaluation of Blood Clearance Rates and  
724 Biodistribution of Poly(2-oxazoline)-Grafted Liposomes. *Journal of Pharmaceutical Sciences* 85,  
725 133-137.

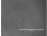
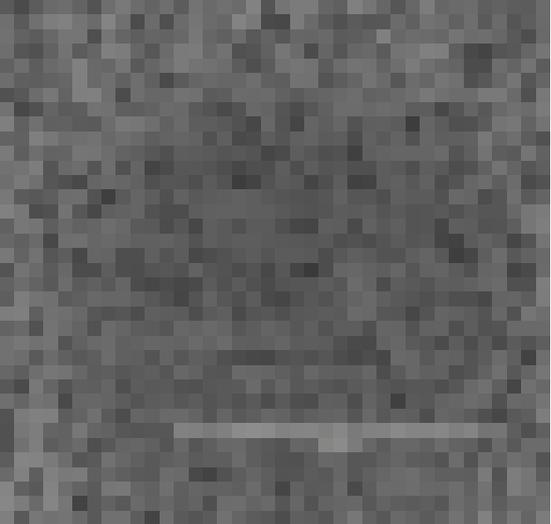
726

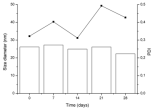
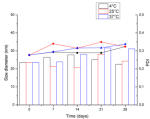
727

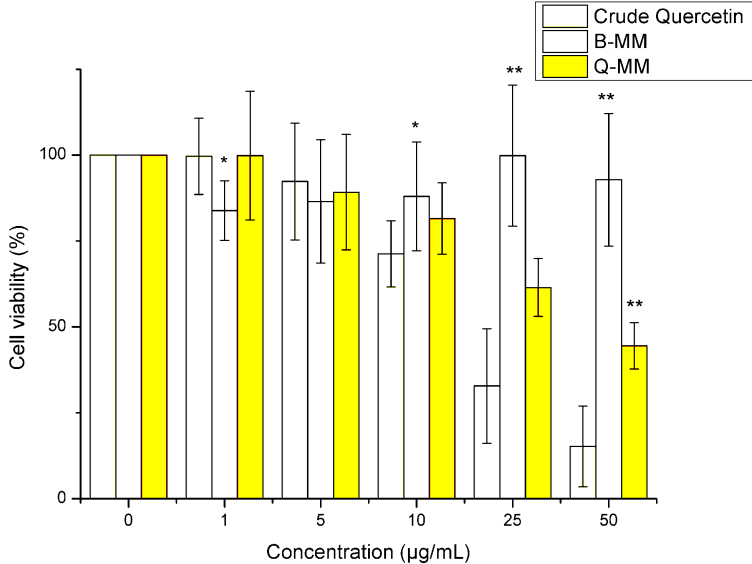


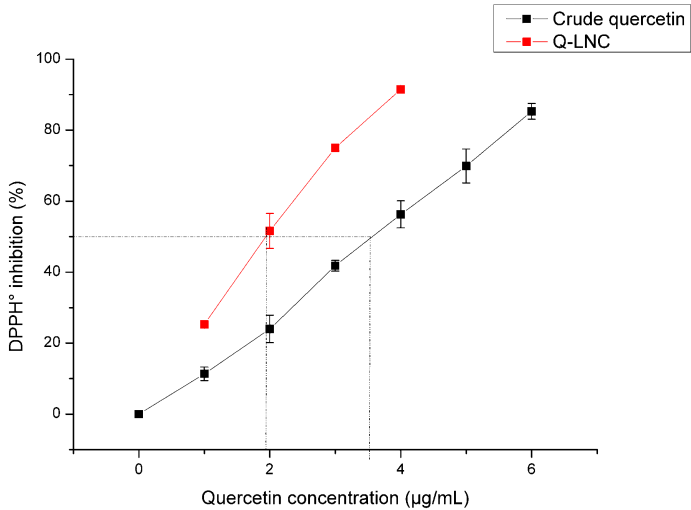


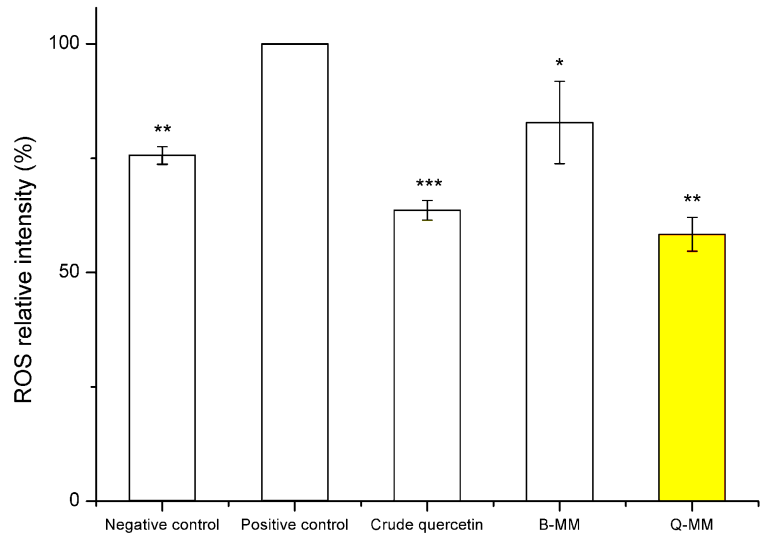












Formulations	B-MM	Q-MM
Particle diameter (nm)	18±2	19±2
PDI	0.30±0.02	0.28±0.01
Zeta potentiel (mV)	0.05±0.08	0.03±0.05

